NATIONAL ADVISORY COMMITTEE FOR AERONAUTICS

TECHNICAL NOTE 2985

A FLIGHT INVESTIGATION OF THE EFFECT OF STEADY ROLLING ON THE NATURAL FREQUENCIES OF A BODY-TAIL COMBINATION

By Norman R. Bergrun and Paul A. Nickel

Ames Aeronautical Laboratory
Moffett Field, Calif.

Washington
August 1953

ERRATA

NACA TN 2985

A FLIGHT INVESTIGATION OF THE EFFECT OF STEADY ROLLING ON THE NATURAL FREQUENCIES OF A BODY-TAIL COMBINATION

By Norman R. Bergrun and Paul A. Nickel
August, 1953

---

1. In figure 8, sublegend 8(a) should read "short-period oscillation" and sublegend 8(b) should read "long-period oscillation."

2. In the title of figure 9, $\frac{I_y}{S\bar{c}} = \frac{I_z}{S\bar{c}} = 7$ instead of 1/7.

NATIONAL ADVISORY COMMITTEE FOR AERONAUTICS

TECHNICAL NOTE 2985

A FLIGHT INVESTIGATION OF THE EFFECT OF STEADY ROLLING ON THE NATURAL FREQUENCIES OF A BODY-TAIL COMBINATION

By Norman R. Bergrun and Paul A. Nickel

SUMMARY

Flight experiments with a freely falling model have been conducted to observe the effects of steady rolling on the pitching and yawing motions of a body-tail combination. Time histories of the pitching and yawing motions show that steady rolling introduces into the pitch oscillations the yawing motions, and into the yaw oscillations, the pitching motions. The observed effects of steady rolling on the values of frequencies are compared with those predicted by theory for damping and for no damping. When damping is included, the calculated frequencies are in good agreement with the observed frequencies, although a good first-order approximation of the frequencies may be obtained by neglecting damping.

Static stability derivatives are assumed for a missile, and it is found that at low speeds and high altitudes, the rolling frequency tends to approach the lower of the body natural frequencies, thereby reducing effective static stability. In addition, graphical relations are presented which permit rapid estimation of changes in the effective static stability derivatives due to steady rolling.

INTRODUCTION

Rolling of an airplane or missile introduces an inertial coupling between the pitching and yawing motions and tends to destabilize the body. This destabilizing effect of rolling becomes more pronounced for aircraft having most of the weight concentrated in the fuselage. Thus, the trend toward use of low-aspect-ratio wings causes the influence of roll on the stability of airplanes and missiles to assume importance.

An analysis of the effect of rolling on stability has been made by Phillips (ref. 1). The principal results are that: (a) For a nonrolling

body, there will be only one frequency of oscillation in the pitching motion and only one frequency in the yawing motion, and the frequencies in pitch or in yaw may be the same or different, depending on the aerodynamic properties of the body; and (b) for a rolling body, there will be two distinct frequencies of oscillation in the pitching motion, and these same two frequencies will appear in the yawing motion; in addition, the faster of the two frequencies will be greater (and the slower of the two will be less) than either the nonroll pitch or yaw frequency. As the roll rate approaches zero, the fast frequency approaches the faster of the nonroll pitch or yaw frequencies, and the slow frequency approaches the slower.

The analysis of reference 1 provides equations for predicting the effect of steady roll on the no-roll natural frequencies in pitch and in yaw. When damping is considered, the equation for the frequencies of oscillation is in the form of a fourth-order polynomial which, ordinarily, is solved by trial and error. When damping is neglected, the fourth-order polynomial derived for the case of damping simplifies to the form of a quadratic equation which can be solved explicitly.

The present investigation was undertaken to provide a free-flight observation of the influence of steady rolling on the frequencies in pitch and yaw of a fuselage-tail combination. The results obtained, when compared with reference 1, would establish the validity of the analysis for the prediction of the effects of rolling on body frequencies.

The fuselage selected for the present investigation had a fineness ratio of 12.4. A roll-stabilization system was employed to maintain the rate of roll at a selected value. The frequency data were obtained by disturbing the model abruptly in pitch and recording the resultant oscillations. The Mach number range of the tests was 0.9 to 1.1.

The tests were conducted at Edwards Air Force Base by personnel from Ames Aeronautical Laboratory of the NACA.

SYMBOLS

a,b,c,d,e dimensionless coefficients of a polynomial having the form

$aD^4 - bD^3 - cD^2 - dD - e$ in which

$a = 1$

$b = 2\zeta_\psi\omega_\psi + 2\zeta_\theta\omega_\theta$

$c = 2 + \omega_\psi^2 + \omega_\theta^2 + 2\zeta_\theta\omega_\theta 2\zeta_\psi\omega_\psi$

$d = 2\zeta_\theta\omega_\theta\omega_\psi^2 + 2\zeta_\theta\omega_\theta + 2\zeta_\psi\omega_\psi\omega_\theta^2 + 2\zeta_\psi\omega_\psi$

$e = 1 + \omega_\theta^2\omega_\psi^2 - \omega_\psi^2 - \omega_\theta^2 + 2\zeta_\psi\omega_\psi 2\zeta_\theta\omega_\theta$

D is a differential operator

a_x, a_y, a_z	longitudinal, lateral, and normal accelerations, g's
$\bar{c}$	mean aerodynamic chord of a reference wing, ft
f_θ	frequency in pitch under conditions of no roll, cps
f_θ'	frequency applicable to a mode of oscillation which approaches the pitching oscillation as the rate of roll approaches zero, cps
f_ψ	frequency in yaw under conditions of no roll, cps
f_ψ'	frequency applicable to a mode of oscillation which approaches the yawing oscillation as the rate of roll approaches zero, cps
I_x, I_y, I_z	moments of inertia about the x,y, and z body axes, respectively, slug-ft^2
M	Mach number
p	rolling velocity, radians/sec
p_t	total pressure, in. Hg
q_o	dynamic pressure, $\frac{1}{2}\rho V^2$, lb/sq ft
q	pitching velocity, radians/sec
r'	ordinate of fuselage, in.
r	yawing velocity, radians/sec
S	exposed area of a reference wing, sq ft
t	time, sec
V	free-stream velocity, ft/sec
α	angle of attack, deg
β	angle of sideslip, deg
δ_h	horizontal-tail deflection, deg
δ_v	vertical-tail deflection, deg
ρ	atmospheric density, slugs/cu ft

ζ_θ fraction of critical damping in pitch of nonrolling body, $-\frac{M_q}{2\omega_\theta p I_y}$, dimensionless

ζ_ψ fraction of critical damping in yaw of nonrolling body, $-\frac{N_r}{2\omega_\psi p I_z}$, dimensionless

ω_θ ratio of no-roll natural frequency in pitch to steady rolling frquency, $\frac{f_\theta}{p/2\pi}$, dimensionless

ω_ψ ratio of no-roll natural frequency in yaw to steady rolling frequency, $\frac{f_\psi}{p/2\pi}$, dimensionless

C_m pitching-moment coefficient of complete model about center of gravity, $\frac{\text{moment}}{q_o S \bar{c}}$, dimensionless

C_{m_α} longitudinal stability derivative for no roll, $-\frac{(2\pi f_\theta)^2 I_y}{q_o S \bar{c}}$, per radian

C_{m_α}' effective longitudinal stability derivative applicable to a mode of oscillation which approaches the pitching oscillation as the rate of roll approaches zero, $-\frac{(2\pi f_\theta')^2 I_y}{q_o S \bar{c}}$, per radian

C_{m_q} $\frac{\partial C_m}{\partial(q\bar{c}/2V)}$, per radian

C_n yawing-moment coefficient of complete model about center of gravity, $\frac{\text{moment}}{q_o S \bar{c}}$, dimensionless

C_{n_β} lateral stability derivative for no roll, $\frac{(2\pi f_\psi)^2 I_z}{q_o S \bar{c}}$, per radian

C_{n_β}' effective lateral stability derivative applicable to a mode of oscillation which approaches the lateral oscillation as the rate of roll approaches zero, $\frac{(2\pi f_\psi')^2 I_z}{q_o S \bar{c}}$, per radian

C_{n_r} $\frac{\partial C_n}{\partial(r\bar{c}/2V)}$, per radian

M_q $C_{m_q}\left(\frac{\bar{c}}{2V}\right) q_o S\bar{c}$, lb-ft-sec/radian

N_r $C_{n_r}\left(\frac{\bar{c}}{2V}\right) q_o S\bar{c}$, lb-ft-sec/radian

DESCRIPTION OF EQUIPMENT

Test Body

The test body was a wingless configuration having a fuselage of fineness ratio 12.4. Figures 1 and 2 show, respectively, a drawing and a photograph of this configuration. Specification of other physical properties is given in table I.

Both the horizontal- and vertical-tail surfaces were all-movable, pivoting on axes perpendicular to the fuselage axis. For horizontal-tail movement, a schedule could be preset so that the tail-fins would deflect and return to trim position in rapid pulse-type movements at designated time intervals during the test phase of the drop. The vertical-tail surfaces were actuated differentially to provide roll control. All tail surfaces were constructed of solid aluminum alloy.

Roll Stabilization

For the tests of this investigation, two different methods were used to obtain the desired roll stabilization. One method consisted of roll-attitude control of the body for the tests in which the roll rate was intended to be nominally zero. The other method consisted of roll-rate control and was used for those tests in which roll rate was to be different from zero. Because of mechanical difficulties, this latter system unavoidably permitted a slight increase in roll rate with increased speed. In addition, the system permitted small variations around the nominal value desired. At most, the magnitude of these variations was about ±0.2 radian per second.

Instrumentation

NACA continuously recording flight instruments were used to record the various quantities measured. A listing of the quantities and of the instruments used to measure them is presented in table II.

TEST PROCEDURE

The results presented in this report were obtained during a series of free-fall drops of the test model in which the model was allowed to fall freely at approximately 0° angle of attack. During the test period of the drop, pitch disturbances of the model were produced intermittently over intervals of time varying from 3 to 8 seconds. At the conclusion of the test period for each drop, the model was recovered by the use of a dive brake and parachute.

Five drops of the body-tail combination comprised the test program. Three of these drops were conducted at constant roll rates of nominally 2.0, 3.5, and 4.0 radians per second. The other two were drops at nominally zero roll rate and were conducted to obtain the natural frequencies of the test configuration in pitch and in yaw.

RESULTS AND DISCUSSION

Experimental Effects of Steady-Roll on No-Roll Natural Frequencies

Reference 1 has indicated the possibility of having coupled motions due to steady rolling. One result of the investigation reported herein has been an experimental verification of the existence of these coupled motions, as shown by the example time histories of angle of attack and angle of sideslip in figure 3. The angle-of-attack and sideslip records presented in this figure are representative of the type of curve resulting when a short-period oscillation and a long-period oscillation are superimposed. The long-period oscillation has been represented by a dashed line in figure 3 to make it more readily discernible. The appearance of both oscillations in each angle-of-attack and sideslip record is a result of coupling due to rolling. The long-period oscillation should not be confused with the phugoid oscillation which, for the test model, would have a period much larger than those of figure 3 (of the order of 25 sec).

As predicted by the analysis of reference 1 and as shown by the time histories in figure 3, the presence of steady rolling causes two frequencies instead of one to appear in the pitching motion, and the same two frequencies also appear in the yawing motion. In the non-rolling case, the pitch and yaw frequencies are known as the "body natural frequencies," and, in order to make the following discussion succinct, the fast frequency will be designated arbitrarily the "pitch" frequency, and the slow frequency, the "yaw" frequency. Similarly, in the subsequent analysis of the rolling case, the fast component of the pitching and yawing frequencies will be referred to arbitrarily as the "pitch"

frequency and the slow component as the "yaw" frequency. In this sense, the presence of steady rolling can be said to have an effect upon the body natural frequencies. This effect is confirmed by experimental data presented in figure 4. Figure 4(a) indicates that as roll rate increased, the frequency in pitch also increased, and figure 4(b) indicates that the frequency in yaw decreased when roll rate was increased. In fact, in one instance, the yaw frequency decreased to zero at some roll rate ranging from about 3.0 to 4.0 radians per second for a condition of low Mach number ($M \approx 0.86$).

The instance of body instability indicated in figure 4(b) is shown in time history form in figure 5. For this test, the roll-control system was programmed to stabilize the model at zero roll rate for 24 seconds, and then to increase the roll rate to a constant value of 4.0 radians per second. At $t = 20.6$ seconds, the body was pulsed in pitch, and, while the body was still oscillating because of the pulse, a change to the 4.0 radian per second roll rate was initiated. At a roll rate in the neighborhood of 3.5 radians per second, an apparent divergence began in the long-period component of pitch and yaw oscillations. Since roll rate was the only factor sensibly changed at the approximate time of divergence, the resulting instability is attributed to the equality of the roll frequency with the lower of the two body natural frequencies. For example, figure 5 indicates that the cyclic roll frequency is approximately 0.56 cycle per second ($3.5/2\pi$) for the Mach number at which divergence occurred. In comparison, the lower of the two natural frequencies at the same Mach number is estimated to be about 0.5 cycle per second (fig. 4(b)).

Comparison of Measured and Experimental Effects of Steady Rolling on the No-Roll Natural Frequencies

The method developed in reference 1 for computing oscillation frequencies, neglecting damping, was employed to compute the frequencies for the test model for the two rates of roll, 2.0 and 3.5 radians per second. The particular equation developed in reference 1 for the calculation of frequencies for no damping ($\zeta_\theta = \zeta_\psi = 0$) is

$$aD^4 - cD^2 - e = 0 \tag{1}$$

where the roots of the equation, after evaluation of the coefficients, provide the results sought. Figure 6 compares the calculated values with the experimental values previously presented in figure 4. As is apparent from the comparison in figure 6, some difference exists between calculated and experimental results, these differences being greatest for the long-period oscillations. Because of these apparent differences, the question is raised as to whether the differences are due to the omission of damping.

The method of reference 1 can be used also to calculate the frequencies of oscillation for the presence of damping. The particular equation developed in reference 1 to calculate oscillation frequencies for presence of damping is a quartic

$$aD^4 - bD^3 - cD^2 - dD - e = 0 \tag{2}$$

Roots of the quartic, after evaluation of the coefficients, provide values of the frequencies sought. The results of calculations using equation (2) are presented in figure 7 where a comparison is made with the experimental data for roll rates of 2.0 and 3.5 radians per second. By comparison of figure 7 with figure 6, the effect of including damping in the calculations is seen to have improved, in general, the agreement between calculated and experimental frequencies. This improvement appears particularly pronounced in the long-period oscillation for a roll rate of 3.5 radians per second. Values of damping used in the computations were small, being in the order of $\zeta_\theta = 0.06$ and $\zeta_\psi = 0.04$ for a roll rate of 2.0 radians per second, and $\zeta_\theta = 0.09$ and $\zeta_\psi = 0.06$ for a roll rate of 3.5 radians per second.

Effects of Roll as Applied to the Design of Missiles

The designer usually thinks of the natural frequencies of an aircraft in pitch and yaw in terms of the static stability parameters C_{m_α} and C_{n_β} where

$$C_{m_\alpha} = -\frac{(2\pi f_\theta)^2 I_y}{q_o S \bar{c}} \tag{3}$$

and

$$C_{n_\beta} = \frac{(2\pi f_\psi)^2 I_z}{q_o S \bar{c}} \tag{4}$$

The effect of steady rolling on these parameters may be considered to modify the nonrolling frequencies (f_θ and f_ψ) to new frequencies (f_θ' and f_ψ') having values dependent upon the rate of roll. The stability parameters which are considered as being effective for the rolling case, therefore, are C_{m_α}' and C_{n_β}'. These effective stability parameters are obtained by replacing f_θ and f_ψ in equations (3) and (4) with f_θ' and f_ψ'. A factor of interest to the designer is the ratios $C_{m_\alpha}'/C_{m_\alpha}$ and C_{n_β}'/C_{n_β}, which represent the ratio of the stabilities during steady rolling to those prevailing at no roll.

In order to provide a rapid method for the determination of the ratios $C_{m_\alpha}'/C_{m_\alpha}$ and C_{n_β}'/C_{n_β} for a wide range of pitching, yawing, and rolling frequencies, two charts based on equation (1) have been prepared, and these are presented in figure 8 for $I_x = 0$ and $I_y = I_z$. Equation (1) neglects damping but provides the first-order effects of steady roll on the no-roll frequencies as evidenced in the present tests. Use of the charts of figure 8 requires knowledge only of the parameters ω_θ^2 and ω_ψ^2 which, for a particular body and roll rate, define a single point in each of figures 8(a) and 8(b). In this regard, the curves of figure 8(a) are drawn for short-period oscillations, and the curves of figure 8(b) for long-period oscillations; that is, when $f_\theta > f_\psi$ (short-period oscillation in pitch, long-period oscillation in yaw), values of $C_{m_\alpha}'/C_{m_\alpha}$ are given by figure 8(a) and values of C_{n_β}'/C_{n_β} are given by figure 8(b). Conversely, when $f_\theta < f_\psi$ (long-period oscillation in pitch, short-period oscillation in yaw), values of $C_{m_\alpha}'/C_{m_\alpha}$ are given by figure 8(b) and values of C_{n_β}'/C_{n_β} are given by figure 8(a). Important regions of instability are labeled in figure 8(b).

The charts of figure 8 have been used to estimate the effects of roll rate upon the static stability of two hypothetical missiles, one symmetric in pitch and yaw, the other asymmetric. The results are shown in figures 9 and 10, respectively, as functions of Mach number and altitude. For the symmetrical missile, the assumed static stability derivatives for no roll are given in figure 9(a) as a function of Mach number. These values were converted to frequencies, and then the parameter, ω_θ^2, was formed for roll rates of 2.0 and 4.0 radians per second. This parameter was used to obtain, from figure 8, values of the factors $C_{m_\alpha}'/C_{m_\alpha}$ and C_{n_β}'/C_{n_β}, applicable to the short- and long-period oscillations for steady rolling. The factors obtained are shown in figures 9(b) and 9(c) for the short- and long-period oscillations, C_{m_α} and C_{n_β}, respectively. For C_{m_α}, all values of the factors obtained are greater than unity; but, in general, the reverse is true for C_{n_β} with values of the multiplying factor C_{n_β}'/C_{n_β} becoming as small as zero.

A set of curves similar to those in figures 9(b) and 9(c) are plotted in figures 10(a) and 10(b) for an asymmetric missile. For this missile, values of C_{m_α} and $I_y/S\bar{c}$ are assumed to be the same as those presented in figure 9(a), but the values of C_{n_β} have been taken arbitrarily as half the values presented in figure 9(a). The factors obtained for the unsymmetrical missile, in general, follow the same trends as the factors obtained for the symmetrical missile. However, for the unsymmetrical missile, values of the factor C_{n_β}'/C_{n_β} can become negative. This condition arises when the solution to equation (1) contains a pair of real roots, and the motion will diverge. Thus, for both symmetric and unsymmetric missiles, steady rolling can be an important factor in reducing static stability. Solutions to equation (1)

indicate that the greatest reduction in static stability is experienced when the roll frequency approaches equality with the lower of the two body natural frequencies. Instances of these reductions in stability are apparent in figures 9(c) and 10(b) ($C_{n_\beta}'/C_{n_\beta} \approx 0$). From these figures it appears that for a given roll rate, the Mach number at which the most reduction in stability occurs increases with increased altitude.

CONCLUSIONS

The results of a series of free-fall-drop tests of a body-tail combination under conditions of systematically varied rates of roll indicate the following conclusions:

1. The tests reported herein have verified experimentally that steady rolling produces coupling of the pitching and yawing motions. In addition, the frequencies of these motions differ from the body natural frequencies.

2. For body-tail combinations having a steady roll rate and body natural frequencies of approximately the same order of magnitude as those measured in the tests of this report, the calculation technique of NACA TN 1627 for no damping may be applied to estimate the first-order effects of steady rolling on body natural frequencies. For a more exact appraisal of this effect, the equations of NACA TN 1627 which include damping should be employed.

3. In accord with theory, a roll frequency which approaches the lower of the two body natural frequencies can cause an unsymmetrical body-tail combination to become statically unstable.

Ames Aeronautical Laboratory
National Advisory Committee for Aeronautics
Moffett Field, Calif., May 27, 1953

REFERENCE

1. Phillips, W. H.: Effect of Steady Rolling on Longitudinal and Directional Stability. NACA TN 1627, 1948.

TABLE I.- PHYSICAL PROPERTIES OF THE TEST MODEL

Body	
Gross weight, lb	1365
I_Y and I_Z, slug-ft^2	800
I_X, slug-ft^2	5
Center of gravity	Station 85.6
Horizontal Tail	
Area (plan form projected to body center line), sq ft	6.0
Aspect ratio (based on plan form projected to body center line), dimensionless	4.4
Taper ratio, dimensionless	0.2
Sweepback, quarter-chord line, deg	45
Span, feet	5.12
Airfoil section, parallel to stream	NACA 65006
Vertical Tail	
Area (plan form projected to body center line), sq ft	3.3
Aspect ratio (based on plan form projected to body center line	5.0
Taper ratio	0.22
Sweepback, quarter-chord line, deg	45
Span, ft	4.05
Airfoil section, perpendicular to quarter-chord line	NACA 65009

TABLE II.- MODEL INSTRUMENTATION

Classification of measurement	Quantity measured	Instrument used
Angles	α β	Slave selsyns recording movements of vanes mounted on boom ahead of body
	δ_h δ_v	NACA 2-component control position recorder
Angular velocities	p q r	NACA single-component turnmeters
Accelerations	a_x a_y a_z	NACA 3-component accelerometer
Pressures	p_o p_t	NACA 6-cell manometer

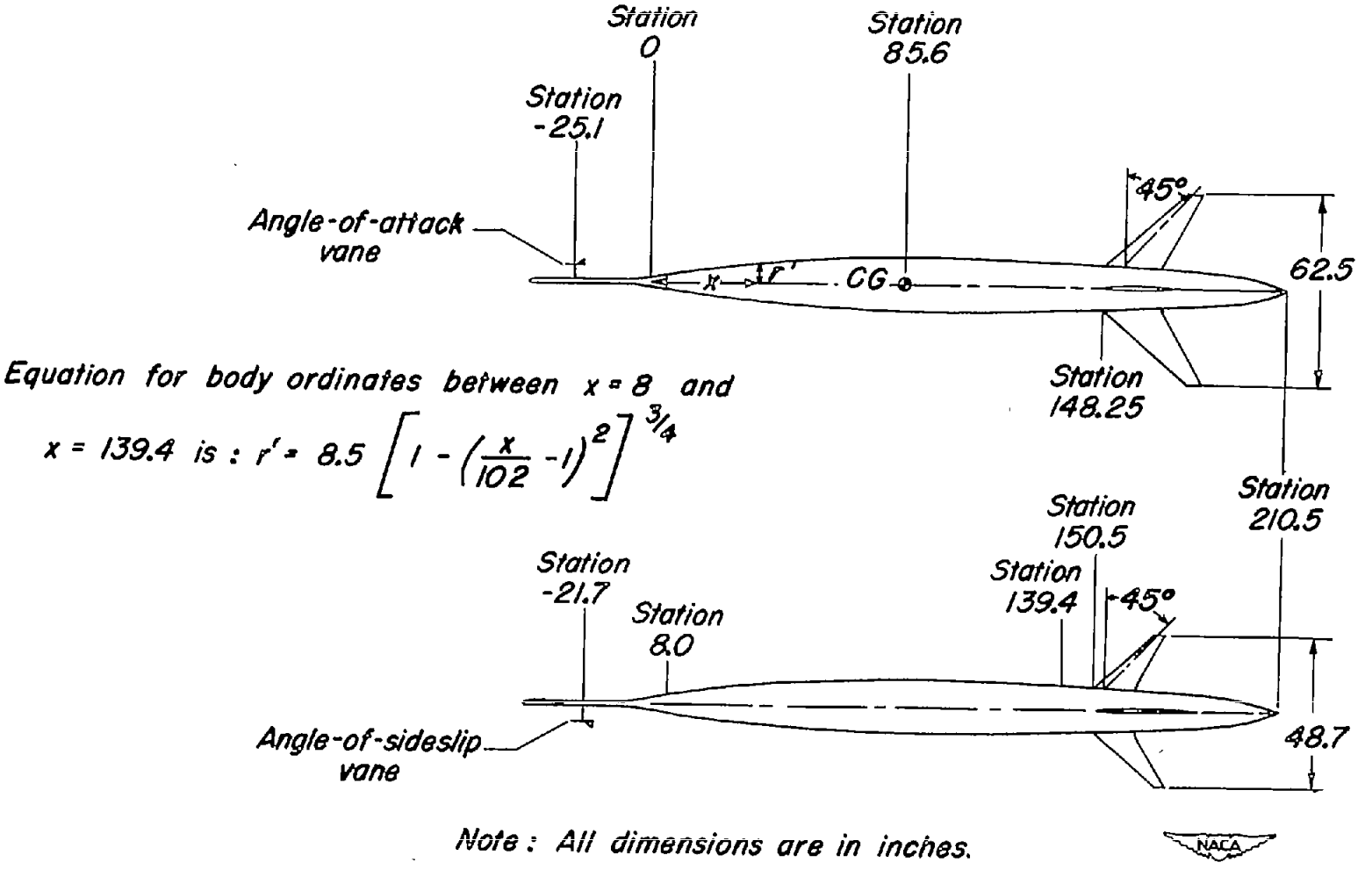

Figure 1.– Geometry and dimensions of test model.

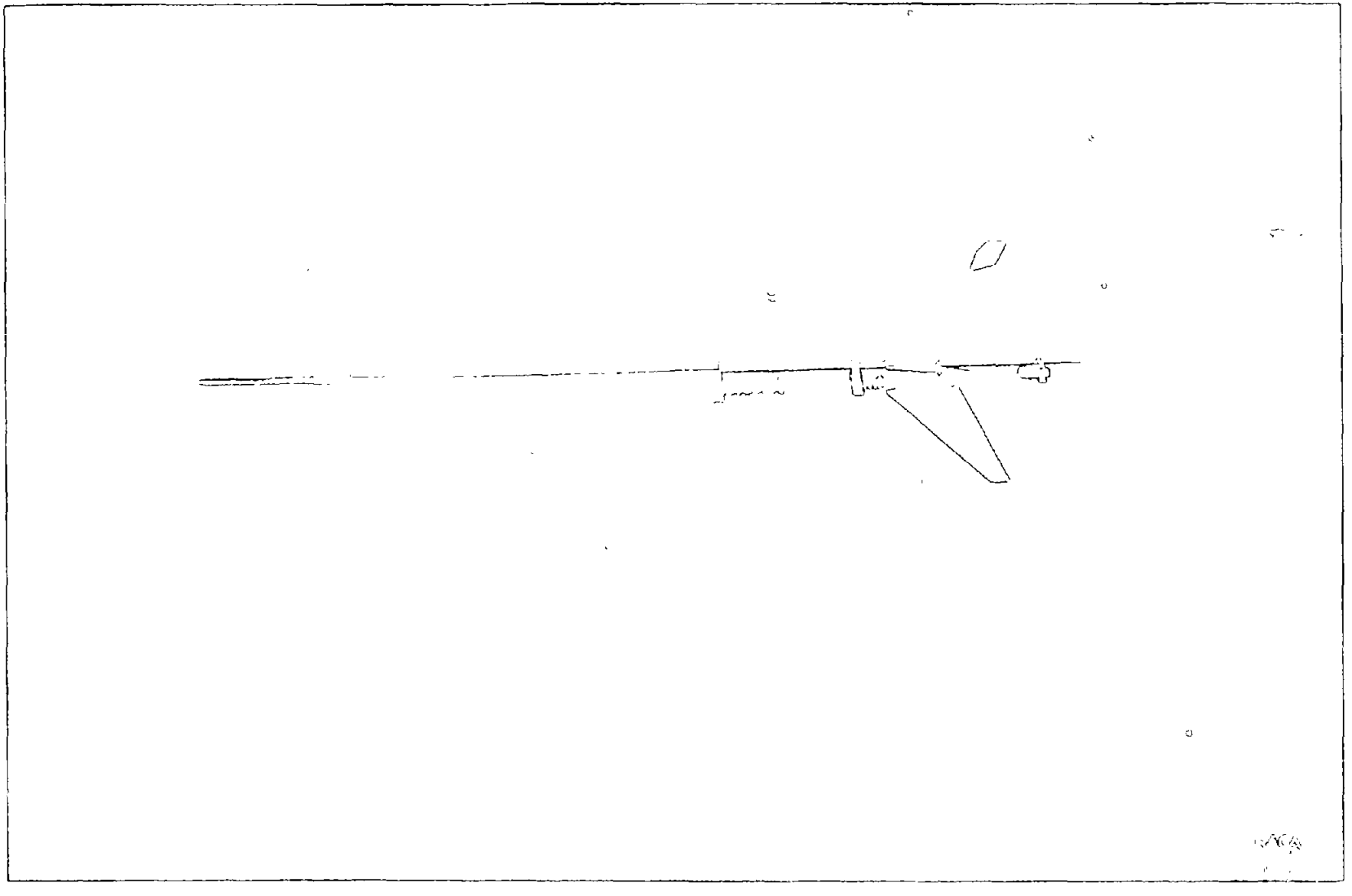

Figure 2.– Test configuration immediately after release from carrier airplane.

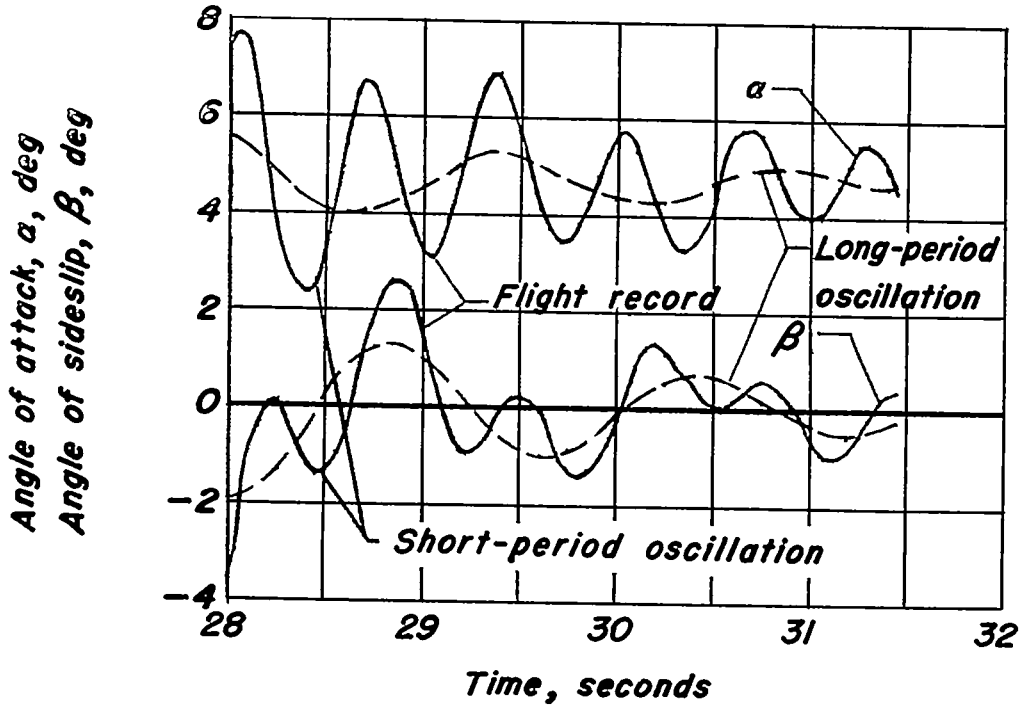

(a) Roll rate, 2.0 radians/sec.

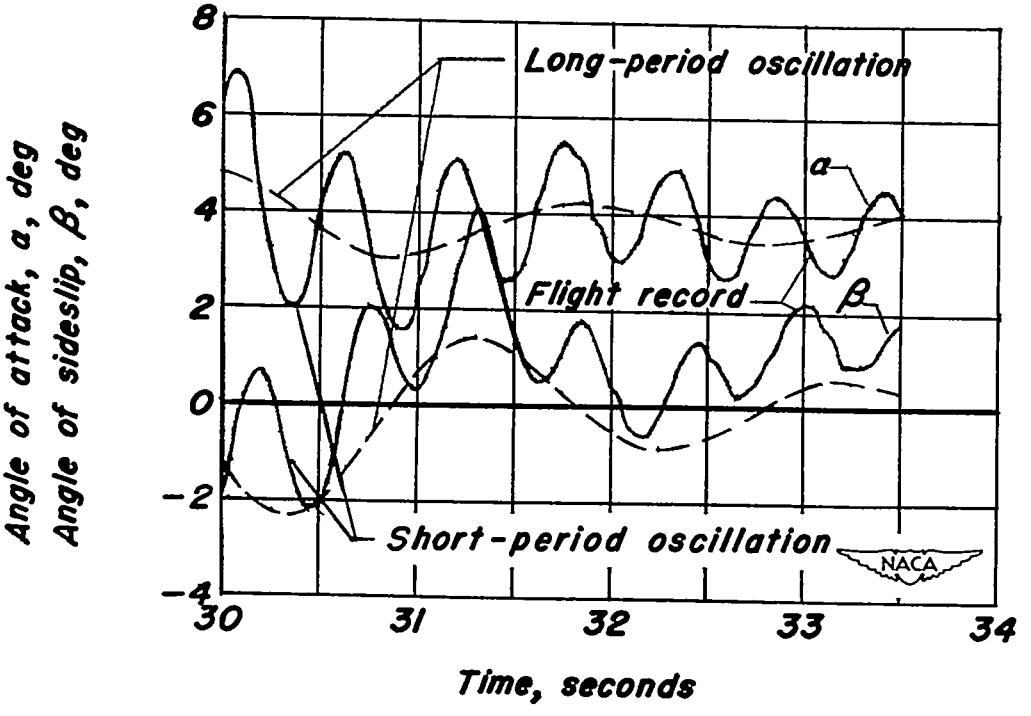

(b) Roll rate, 3.5 radians/sec.

Figure 3.– Time histories of angle of attack and sideslip for comparable Mach number ranges showing existence of coupled frequencies due to rolling.

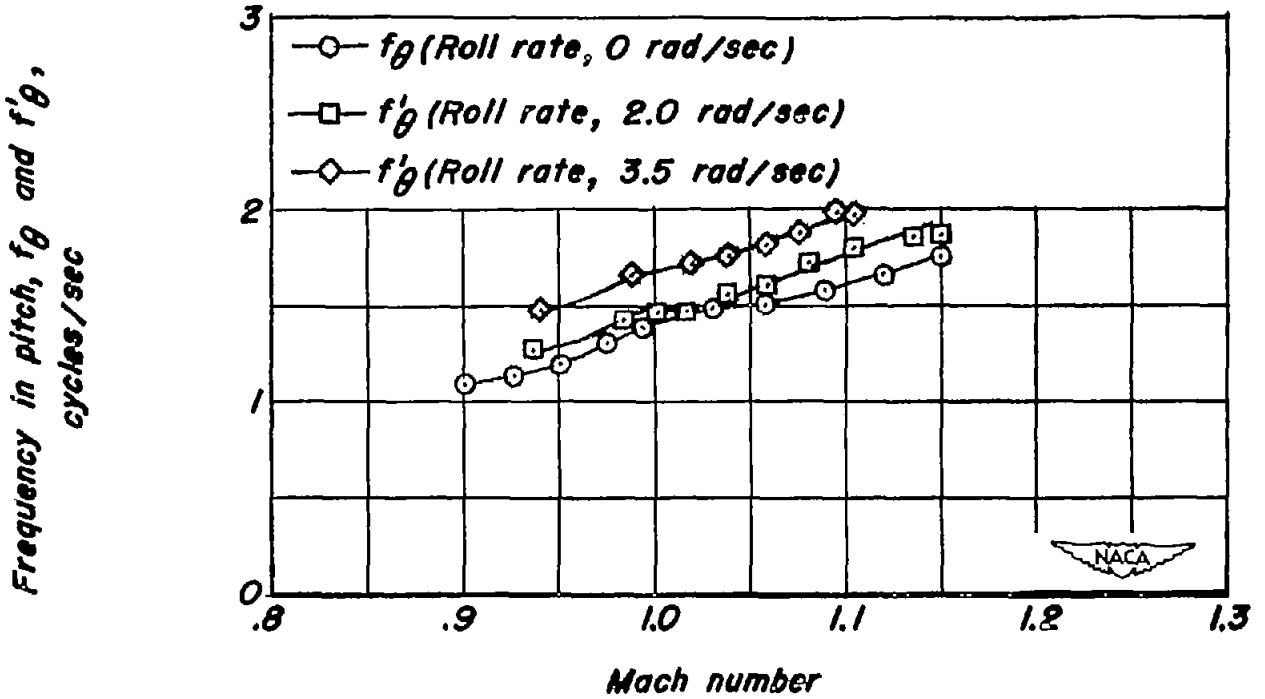

(a) Pitch frequency (short-period oscillation).

Figure 4.– Effect of steady rolling on natural frequencies of the test body.

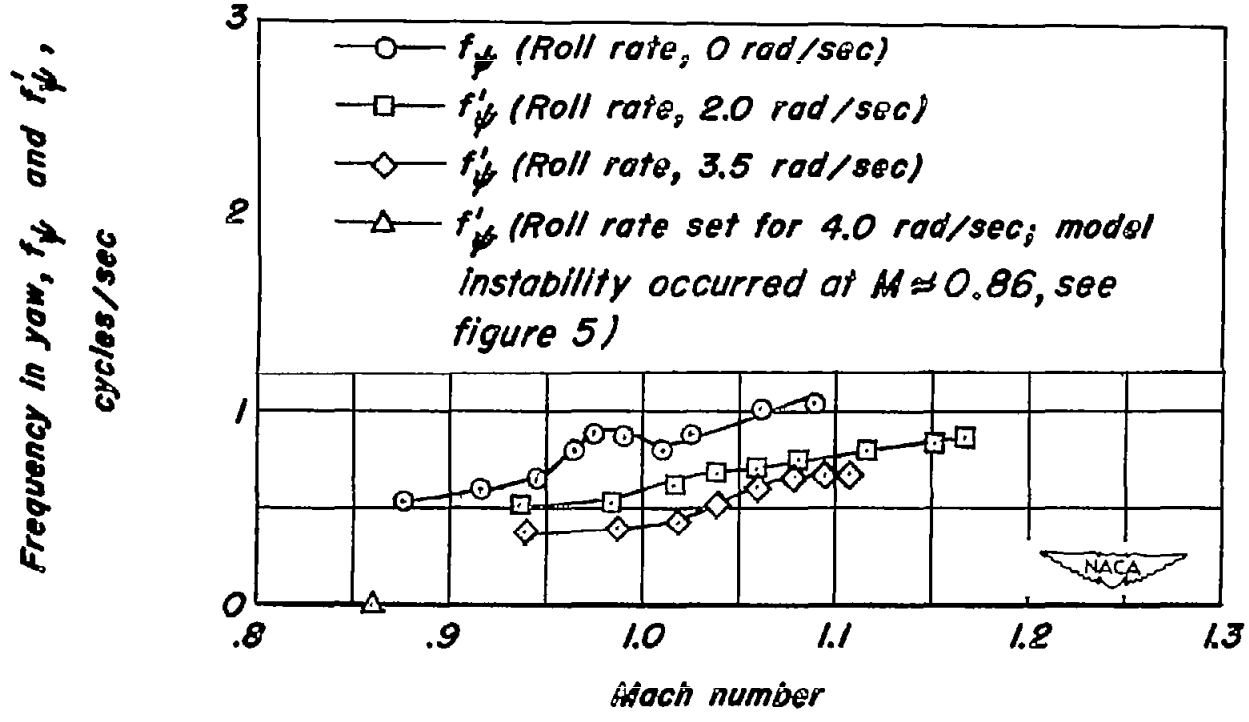

(b) Yaw frequency (long-period oscillation).

Figure 4.– Concluded.

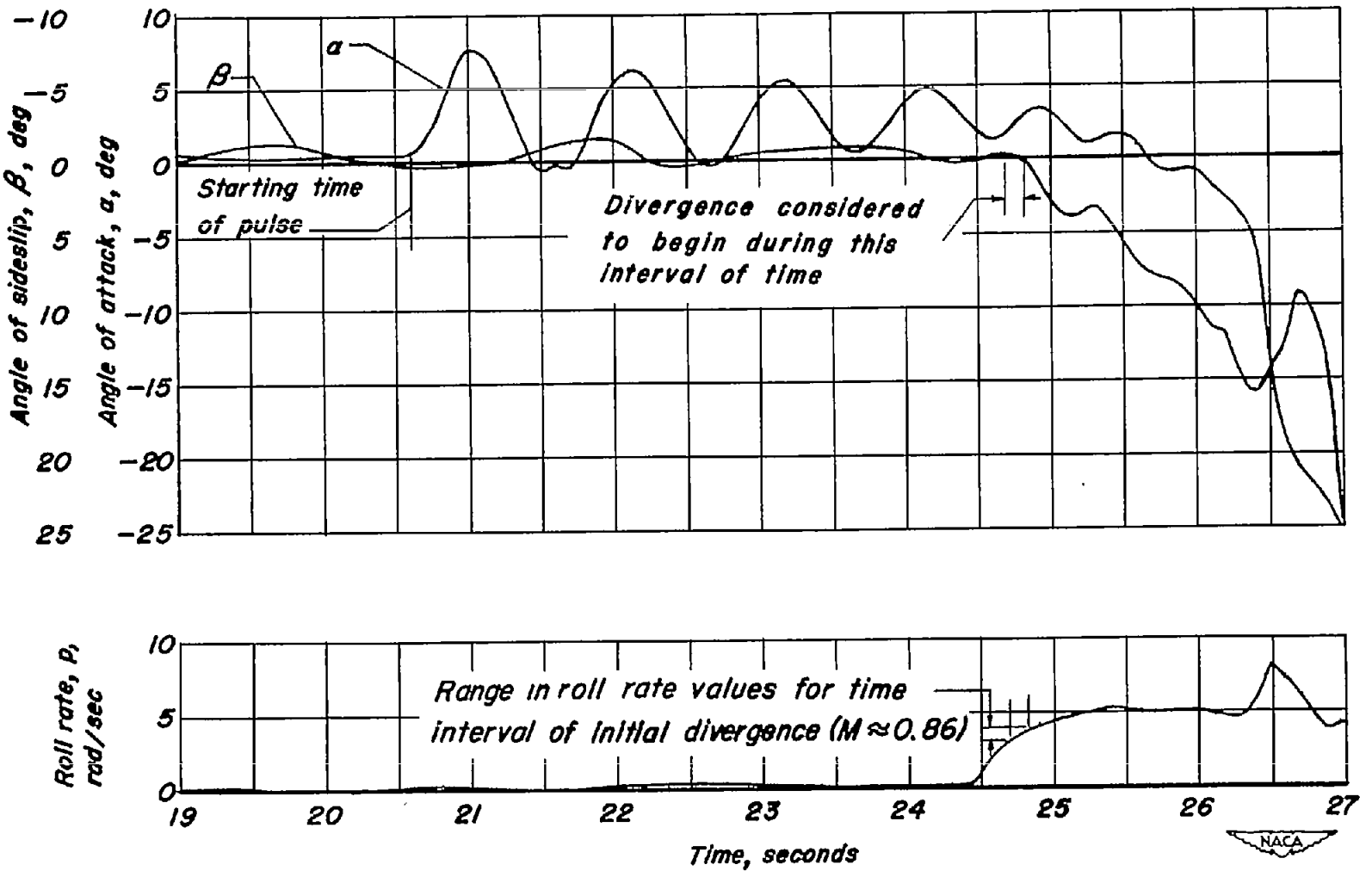

Figure 5.- Time histories for a drop of the test body showing the occurrence of divergence at a roll rate of approximately 3.5 radians/sec.

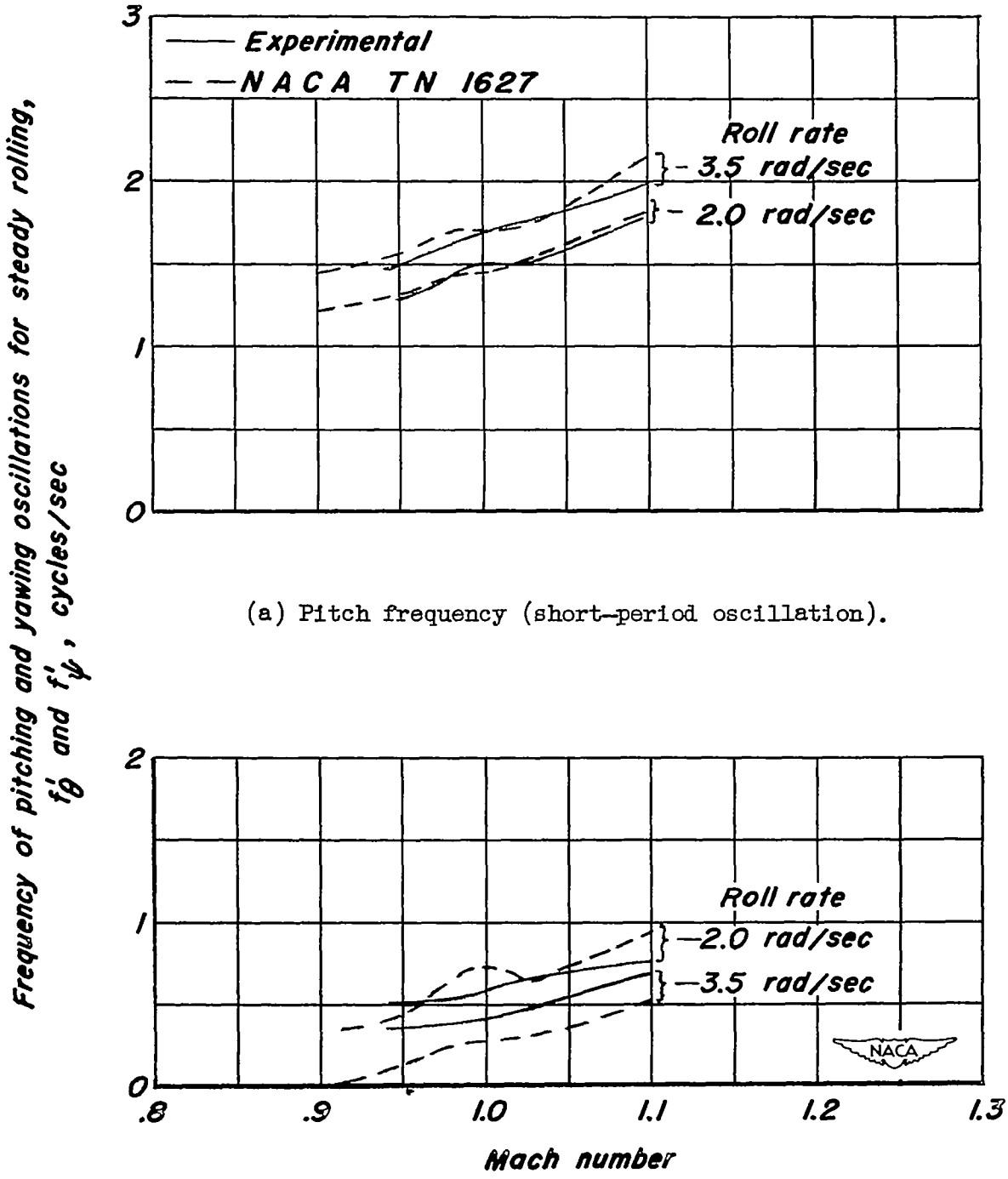

(a) Pitch frequency (short-period oscillation).

(b) Yaw frequency (long-period oscillation).

Figure 6.- Comparison of experimental frequencies with those calculated by the method of NACA TN 1627 for steady rolling and no damping.

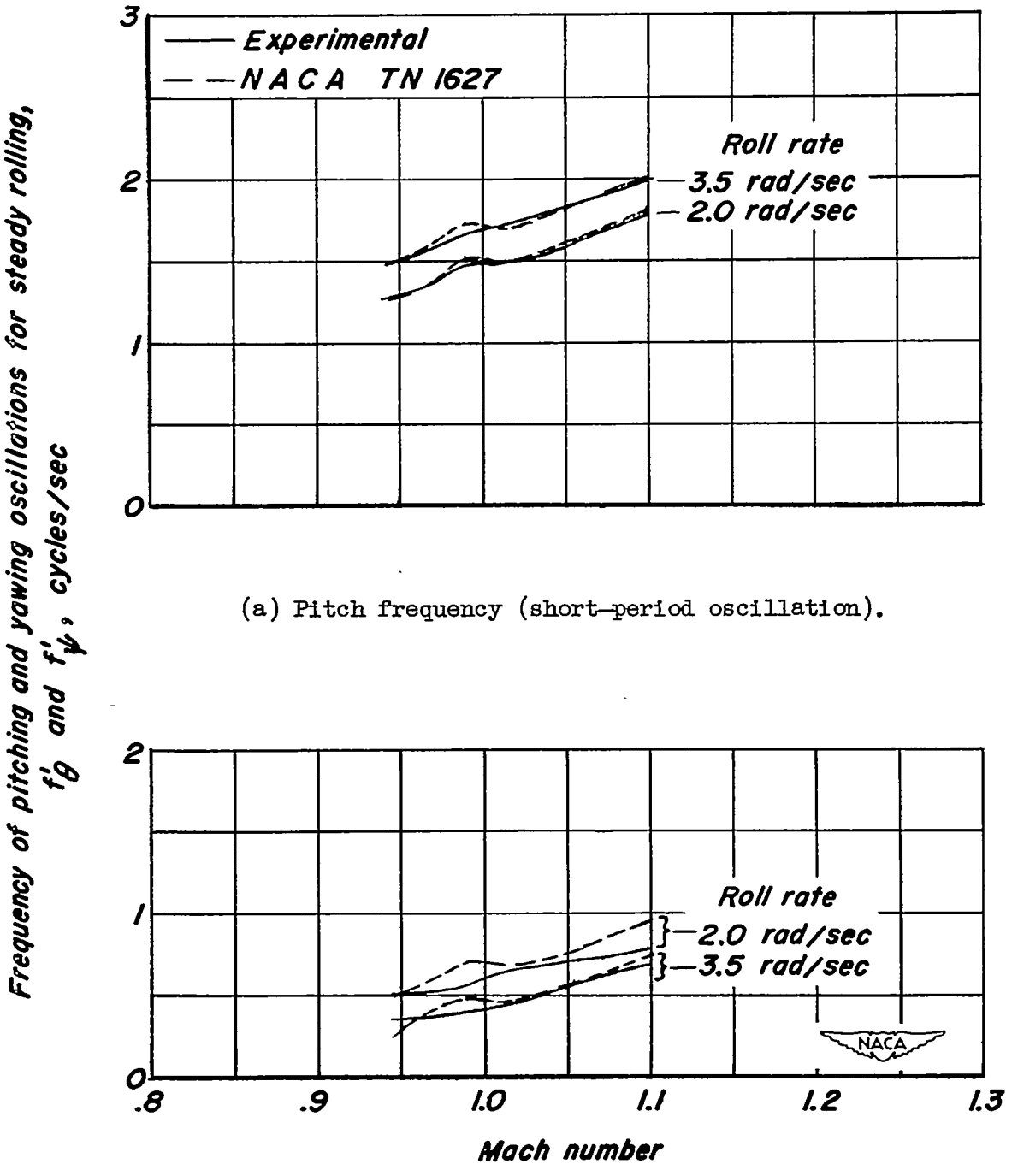

(a) Pitch frequency (short-period oscillation).

(b) Yaw frequency (short-period oscillation).

Figure 7.– Comparison of experimental frequencies with those calculated by the method of NACA TN 1627 for steady rolling, by use of experimentally determined values of damping.

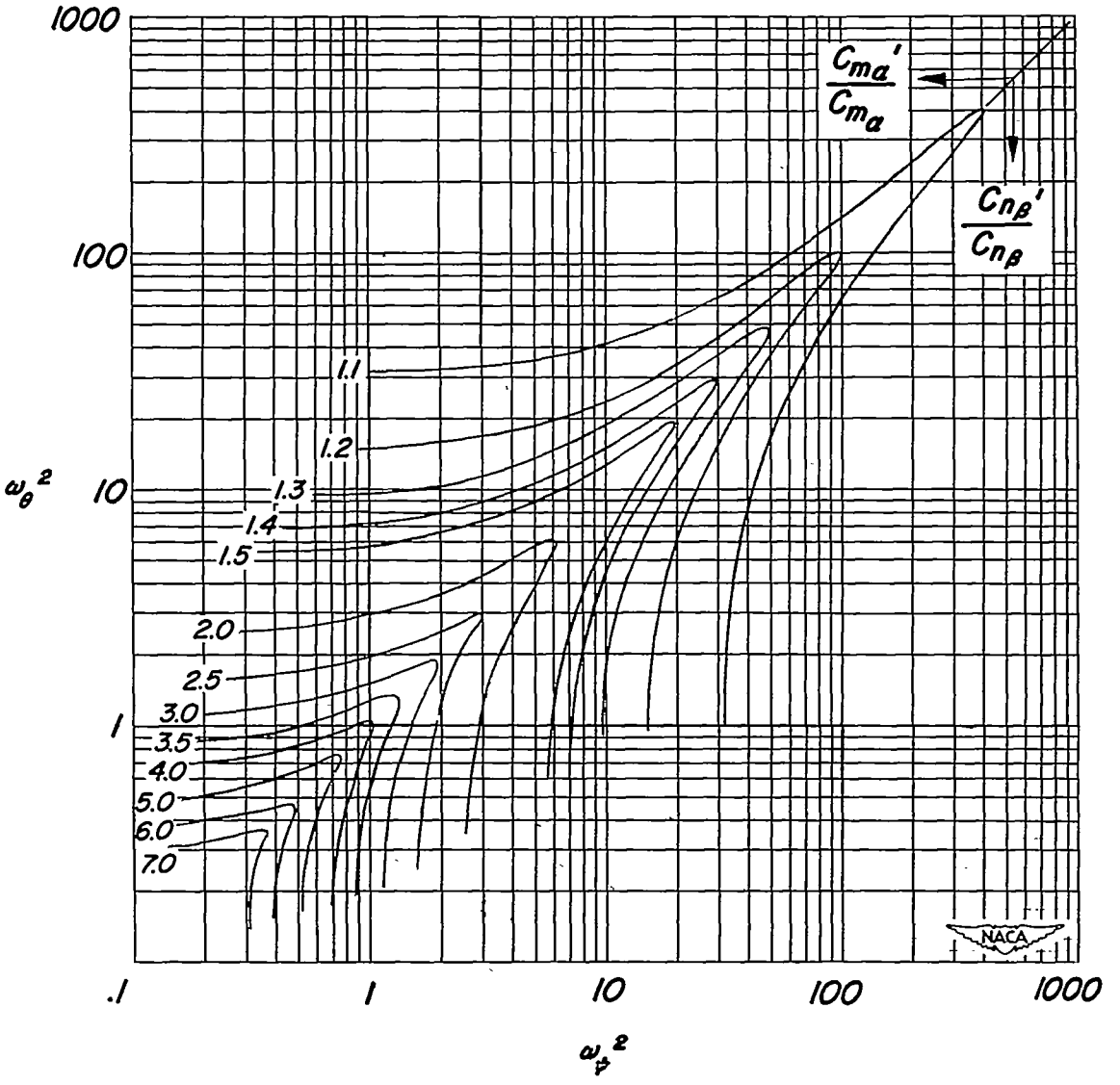

(a) Long-period oscillation.

Figure 8.– Static stability derivative ratios as a function of body natural frequency and roll rate; $\zeta_\theta = \zeta_\psi = 0$.

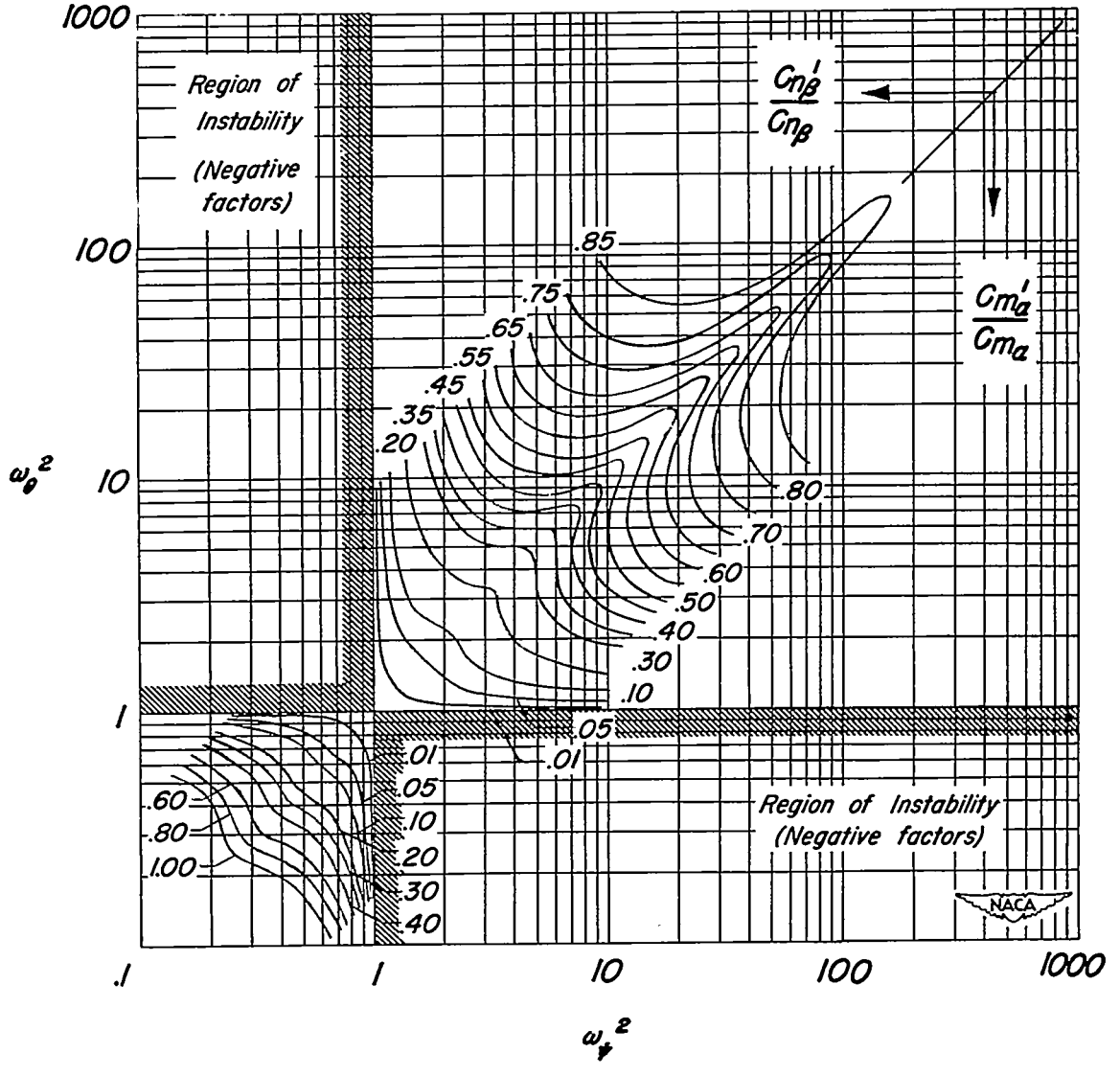

(b) Short-period oscillation.

Figure 8.- Concluded.

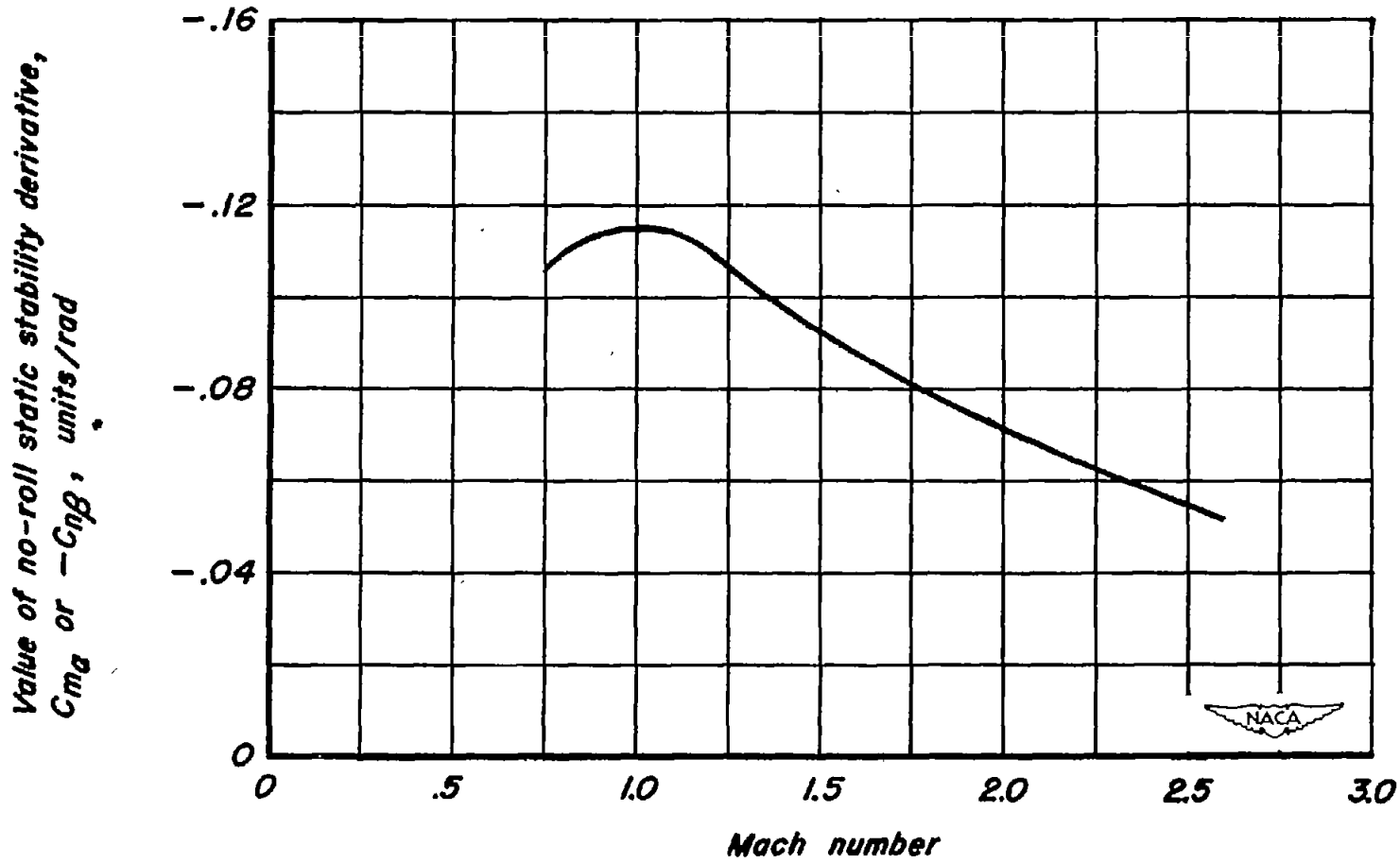

(a) No-roll stability derivatives for lateral and pitch planes.

Figure 9.– Static stability derivatives for a symmetric missile as affected by Mach number, rate of steady rolling, and altitude; $\frac{I_y}{Sc} = \frac{I_z}{Sc} = \frac{1}{7}$.

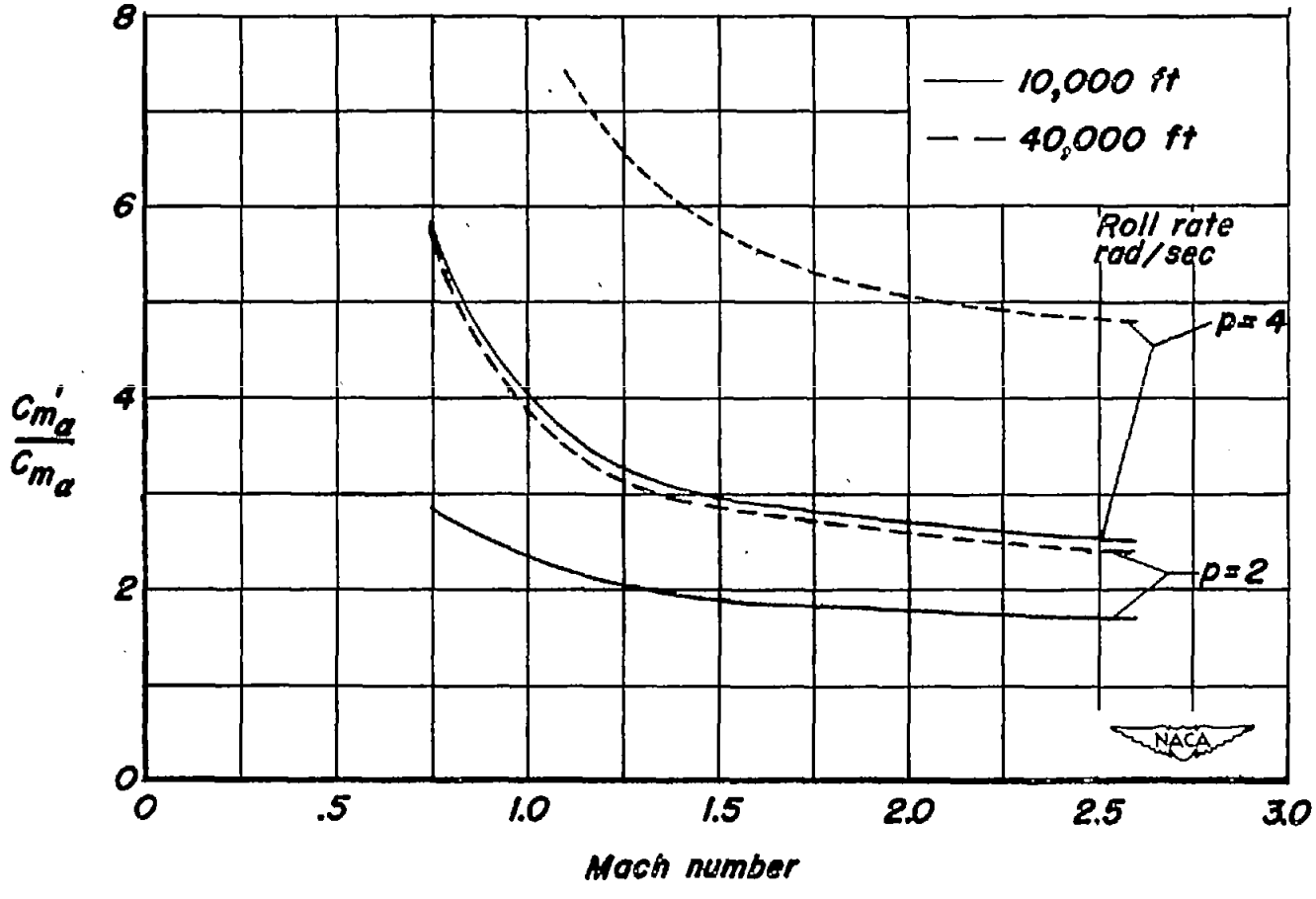

(b) Effect of steady rolling on C_{m_α} when missile is disturbed in pitch; $\zeta_\theta = \zeta_\psi = 0$.

Figure 9.– Continued.

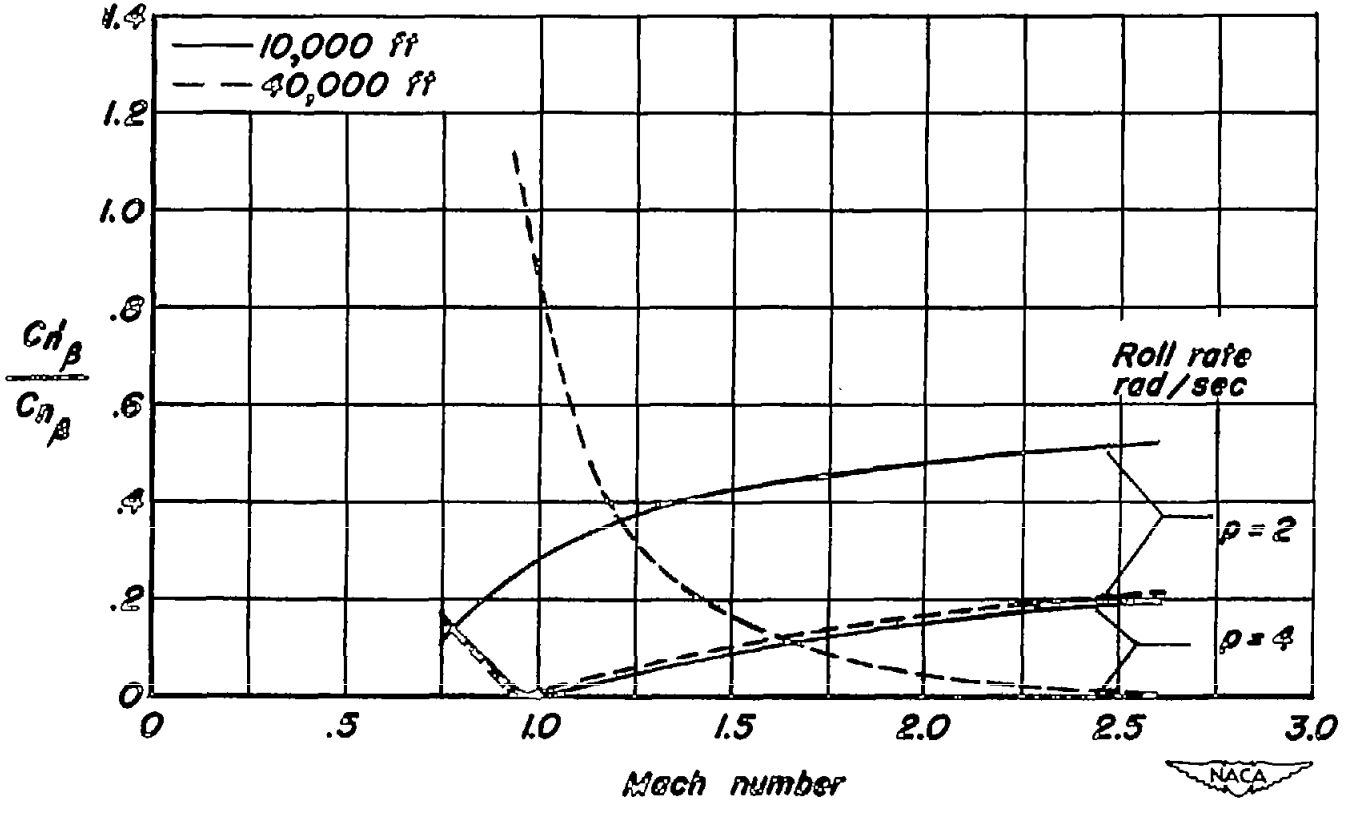

(c) Effect of steady rolling on C_{n_β} when missile is disturbed in pitch; $\zeta_\theta = \zeta_\psi = 0$.

Figure 9.- Concluded.

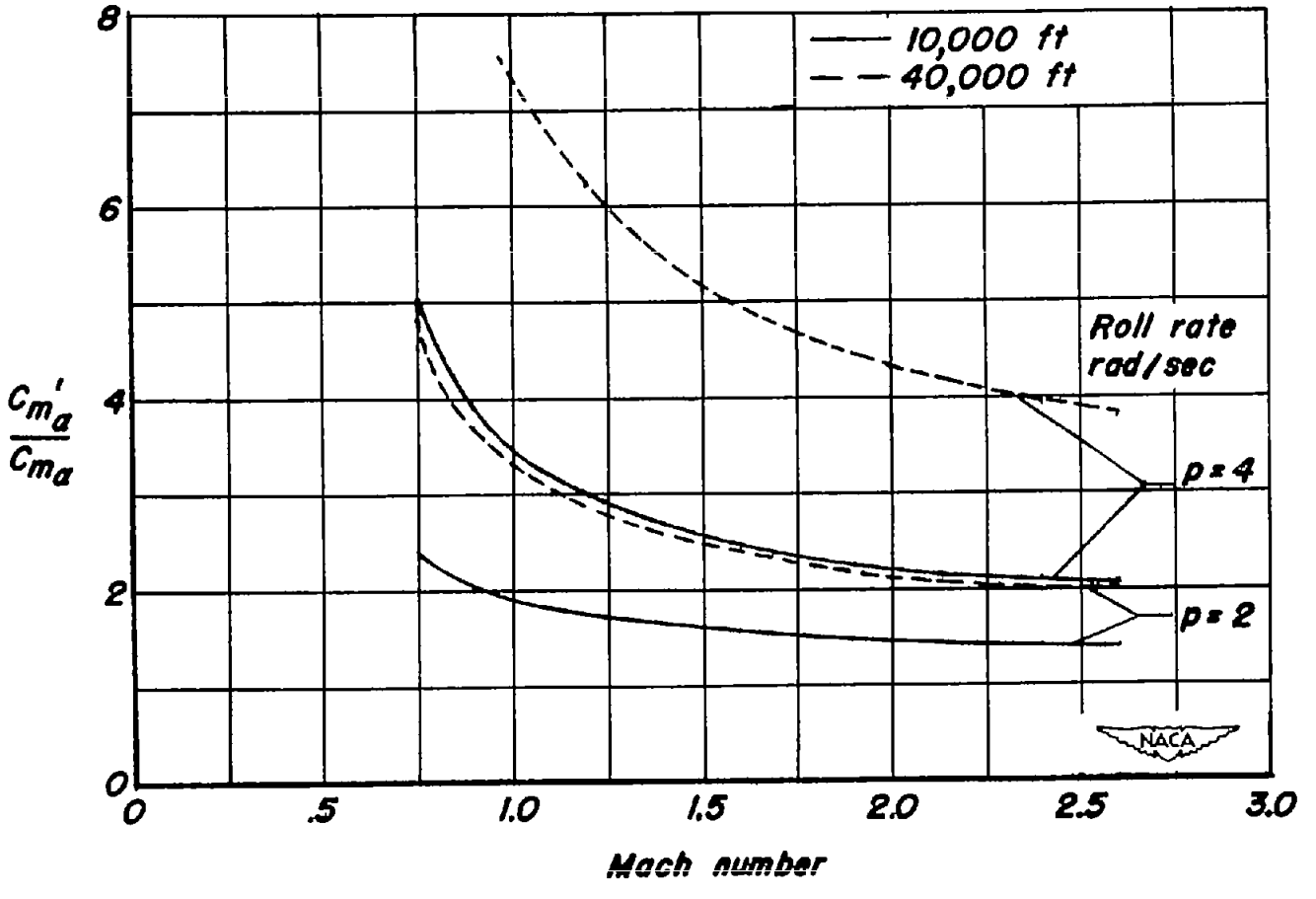

(a) Effect of steady rolling on C_{m_α} when missile is disturbed in pitch.

Figure 10.– Static stability derivatives for a hypothetical unsymmetrical missile as affected by Mach number, rate of steady rolling, and altitude; $\zeta_\theta = \zeta_\psi = 0$.

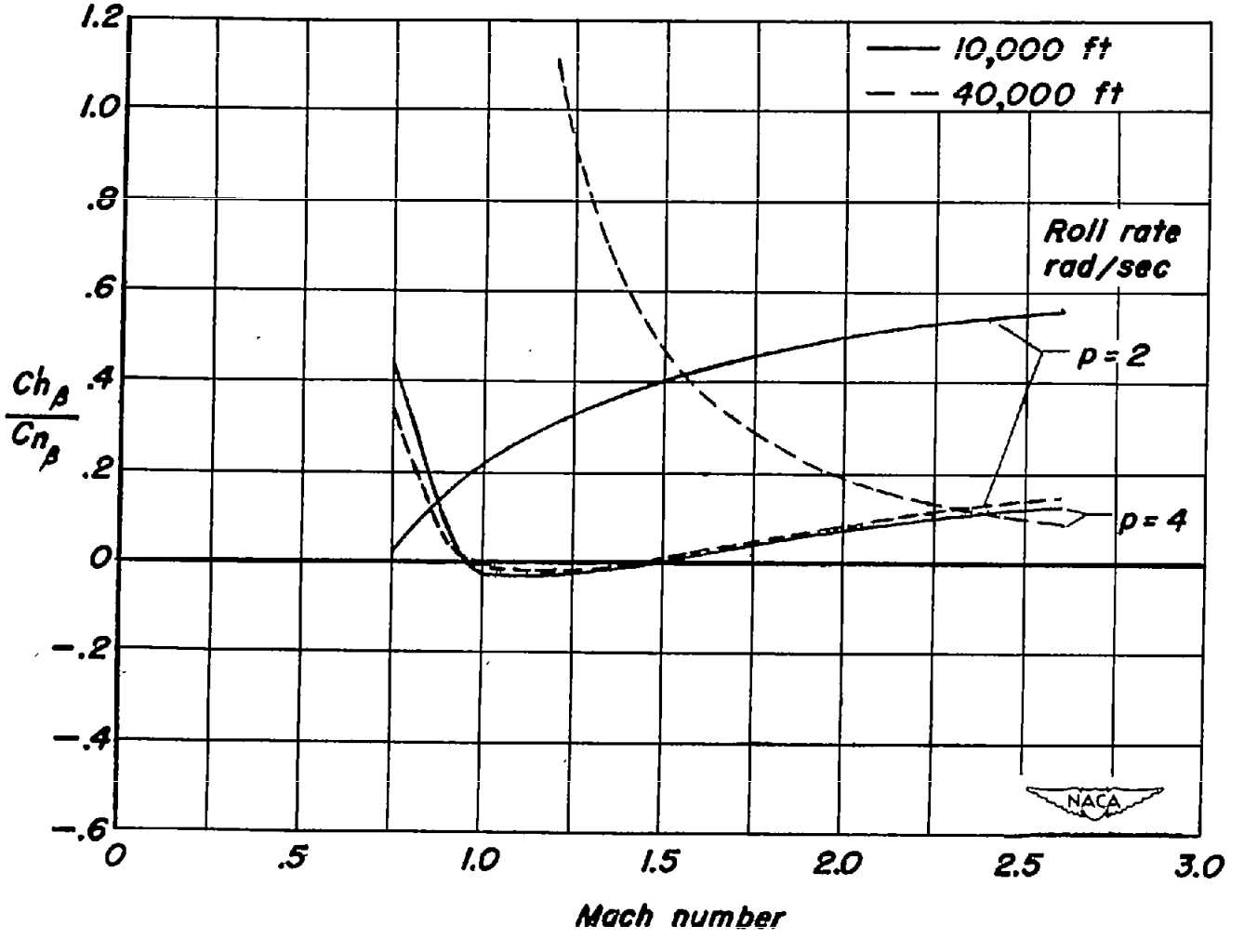

(b) Effect of steady rolling on C_{n_β} when missile is disturbed in pitch.

Figure 10.– Concluded.

NACA-Langley - 8-6-53 - 1000